

Impact production of nitrogen oxides in the Hadean atmosphere

Alan Heays¹, Tereza Kaiserová^{1,2}, Paul Rimmer^{3,4,5}, Antonín Knížek^{1,2}, Lukáš Petera^{1,6}, Svatopluk Civiš¹, Libor Juha^{7,8}, Roman Dudžák^{7,8}, Miroslav Krůs⁸, Manuel Scherf⁹, Helmut Lammer⁹, Robert Pascal¹⁰, and Martin Ferus¹

¹J. Heyrovský Institute of Physical Chemistry, Czech Academy of Sciences, Prague, Czech Republic

²Charles University in Prague, Faculty of Science, Department of Physical and Macromolecular Chemistry, Prague, Czech Republic

³Department of Earth Sciences, University of Cambridge, Cambridge, United Kingdom

⁴Cavendish Astrophysics, University of Cambridge, Cambridge, United Kingdom.

⁵MRC Laboratory of Molecular Biology, Cambridge, United Kingdom.

⁶Charles University in Prague, Faculty of Science, Department of Inorganic Chemistry, Prague, Czech Republic

⁷Department of Radiation and Chemical Physics, Institute of Physics, Czech Academy of Sciences, Prague, Czech Republic

⁸Laser Plasma Department, Institute of Plasma Physics, Czech Academy of Sciences, Prague, Czech Republic

⁹Austrian Academy of Sciences, Space Research Institute, Graz, Austria

¹⁰Laboratoire de Physique des Interactions Ioniques et Moléculaires, Aix-Marseille Université – CNRS, UMR 7345, Marseille, France

Key Points:

- A laboratory model of N_xO_y formation by impacts finds a large yield of N_2O .
- The steady-state abundance of N_2O in a one-dimensional atmospheric model shows that impact-production is still insufficient to significantly warm the Hadean Earth.

Corresponding author: Martin Ferus, martin.ferus@jh-inst.cas.cz

Abstract

We investigate the impact formation of nitrogen oxides in the model Hadean atmosphere and the potential for greenhouse warming due to the production of nitrous oxide (N_2O). N_2O has been considered to be a relatively stable greenhouse gas produced by impact plasma. However, its warming potential strongly depends on its production rate and its stability in the early atmosphere. The high-energy-density synthesis efficiencies of NO , N_2O , and NO_2 are evaluated for gas mixtures representing an early Earth atmosphere by simulating an impact plasma with terawatt-class laser-induced dielectric breakdown (TC-LIDB) using the terawatt-scale Prague Asterix Laser System. Manifestations of laser induced high-energy-density plasma, such as a plasma temperature exceeding 10 000 K, high electron densities and large interaction volume, make this one of the best available laboratory models for simulating the chemical consequences of a meteoroid atmospheric entry. The measured yields of NO , N_2O , and NO_2 have been found to reach 6×10^{16} , 2×10^{16} , and 2×10^{15} molec J^{-1} , respectively. The N_2O yield is far above an upper limit determined from a previous tabletop LIDB experiment, while the NO and NO_2 yields are in broad agreement with a range of LIDB and electric-discharge experiments. Using the yield estimated for TC-LIDB plasma simulating an asteroid impact and a one-dimensional photochemical model of the Hadean atmosphere undergoing heavy bombardment, we find a large source flux of N_2O , but its steady-state partial pressure is still insufficient to warm the climate. These findings support a scenario of early Earth warming by other greenhouse gases, a significant source of N_2O other than impacts, or a relatively cold climate during part of the Hadean eon plausible for lower global temperatures due to anticipated lack of solar flux or depletion of greenhouse gases such as CO_2 on young early Earth.

Plain language summary

The climate of the Earth 4.5 to 4 billion years ago is not well known but geological evidence suggests the presence of liquid water. Although subglacial occurrence of liquid water cannot be excluded, some theories assume that this is at odds with the possibility of a very cold, and perhaps completely frozen, early Earth implied by the less-bright Sun at that time. Extra greenhouse warming of the Earth by atmospheric gases is then thought necessary to keep the surface temperature high enough for liquid water. Meteorites impacted the early Earth at a greater rate than today and provided a source of energy for forming possible greenhouse-gas molecules. In this paper, we mimic the impact-triggered formation of nitrogen oxide molecules (NO , NO_2 , N_2O) in the laboratory using a laser-created high energy plasma. We then compute the stable amount of N_2O that might have existed 4.5 billion years ago and find this to be too small to contribute to greenhouse warming. However, the effect of large amounts of impact-formed nitrogen oxides may be significant for detailed studies of the short-time consequences of a large impact on the early-Earth atmosphere, or as chemical inputs to the first stages of biochemistry, or for models of the atmospheres of exoplanets in young star systems encountering heavy bombardment.

1 Introduction

The geological record of well-preserved rocks from the Hadean eon preceding 4 Ga is lacking and the physical and chemical environment at that time is obscured. This uncertainty encompasses the important transition from a hot and hostile world following the Moon-forming event between 4.51 and 4.47 Ga (Bottke et al., 2015; Lock et al., 2020) and heavy bombardment and late veneer occurring before 3.5 Ga (Genda et al., 2017; Bottke & Norman, 2017) to the hot but life supporting Archean ocean planet established by around 4 Ga (Catling & Zahnle, 2020).

74 Extra-terrestrial impacts certainly influenced the Earth over this period, and the
 75 remnant lunar surface (Koeberl, 2006; Ryder, 2002) implies a decreasing number of im-
 76 pactors with solar system age, with the median estimate for a final impact capable of
 77 global ocean vaporisation of 4.3 Ga (Marchi et al., 2014). Lunar studies (Bottke & Nor-
 78 man, 2017) also suggest Earth experienced a late-heavy bombardment (LHB) with in-
 79 creased impact frequency between 4.2 and 3.5 Ga and peaking at (3.85 ± 0.05) Ga (Koeberl
 80 et al., 2000), but its occurrence and timing are not agreed upon (Wetherill, 1975; Boehnke
 81 & Harrison, 2016; Morbidelli et al., 2018; Mojzsis et al., 2019).

82 Analysis of Ce-anomalies in igneous zircons of crustal origin preceding 4 Ga reveal
 83 a significantly more reduced Hadean continental crust than today, and a progressive ox-
 84 idation between 4 and 3.6 Ga (Yang et al., 2014). This could be the result of massive im-
 85 pact delivery and impact-induced degassing of reduced material (Kuwahara & Sugita,
 86 2015), that is, CO- and H₂-rich volcanic species (Yang et al., 2014) with the probable
 87 addition of CH₄-rich fluids, along with a possible contribution to transient highly-reducing
 88 atmospheric states through the reduction of seawater to hydrogen by iron-cored impactors
 89 (Genda et al., 2017; Zahnle et al., 2020). Overall, the degree to which the atmosphere
 90 was reducing and its precise composition remain unknown, and theorising on the evo-
 91 lution of these parameters over geological time is an active field of research (e.g., Shaw
 92 (2008); Lammer et al. (2018); Zahnle et al. (2020)).

93 Stellar-evolution models maintain that total solar intensity has steadily increased,
 94 with approximately 30% more radiative-energy output today than 4.6 Ga (Feulner, 2012;
 95 Charnay et al., 2020). One dimensional models of radiative transfer in the Archean and
 96 Hadean atmosphere find a lower surface temperature than today to the extent where no
 97 liquid water is expected on the surface (Sagan & Mullen, 1972; Feulner, 2012), in con-
 98 tradiction to analyses of 4 Ga igneous zircons presenting strong evidence for the pres-
 99 ence of liquid water and supracrustal rocks around 4.2 Ga, or possibly as early as 4.325
 100 Ga (Wilde et al., 2001; Cavosie et al., 2005).

101 Some proposed sources for the extra warming needed to prevent a frozen Hadean,
 102 and subsequent Archean eon, are reviewed by Kasting and Catling (2003), Feulner (2012),
 103 and Charnay et al. (2020), and include Solar mass-change, alteration of the Earth’s albedo
 104 by clouds or continental configuration, an enhanced Solar wind flux, or rotation and obliq-
 105 uity variations. The leading hypothesis is enhanced greenhouse warming due to infrared-
 106 active atmospheric molecules, with arguments set forth proposing CO₂ (Kuhn & Kast-
 107 ing, 1983; Kasting & Catling, 2003; Kasting, 2014), NH₃ (Sagan & Mullen, 1972; Kuhn
 108 & Kasting, 1983), and CH₄ (Kiehl & Dickinson, 1987; Haqq-Misra et al., 2008). Inves-
 109 tigators of greenhouse effects in the more-recent Proterozoic atmosphere predict possi-
 110 ble climate forcing due to N₂O (Buick, 2007; Roberson et al., 2011; Stanton et al., 2018)
 111 but require a biologically-mediated source or reasonable O₂ co-abundance that are un-
 112 likely to apply to the Hadean. Alternatively, Airapetian et al. (2016) proposed an en-
 113 hanced Solar wind flux could have increased the abiotic nitrogen N-fixation rate and lead
 114 to an abundance of N₂O. The importance of the species mentioned above to greenhouse
 115 warming hinges on their potential for radiative forcing, source magnitude, and stabil-
 116 ity against photolysis, chemistry, surface deposition, and atmospheric escape. Recently,
 117 three-dimensional global climate models including atmosphere-surface feedback, as re-
 118 viewed by Charnay et al. (2020), find warming of the Archean by an abundance of CO₂
 119 within geological constraints can be sufficient to prevent a global ice age.

120 Another motivation for estimating the early-Earth abundance of N_xO_y species is
 121 to constrain their potential influence on the development of life. The fixation of N₂ makes
 122 available a huge amount of energy following the reaction of NO_x species (NO and NO₂)
 123 with simple prebiotic precursors like cyanate or the derivatives of urea, with the provi-
 124 sion of several hundreds kJ mol⁻¹ estimated from thermodynamic data (Amend & Shock,
 125 2001) In this context, nitric oxide can drive the abiotic formation of peptide biopolymers
 126 from amino acid derivatives (Taillades et al., 1999). Nitric oxide is also a proposed elec-

127 tron acceptor during the evolution of the biochemical metabolisms of aerobic respiration
 128 and oxygenic photosynthesis before atmospheric oxygenation (Ducluzeau et al., 2009;
 129 Gribaldo et al., 2009; Wong et al., 2017).

130 The formation of NO_x by lightning has been well-studied in the laboratory and en-
 131 vironment (e.g., Chameides et al. (1977); Levine et al. (1981); Navarro-González et al.
 132 (2001)). Modern-day lightning produces NO_x at a rate of $2 \times 10^{11} \text{ moly}^{-1}$ (Schumann
 133 & Huntrieser, 2007) out of a total natural and anthropogenic source of $1.4 \times 10^{12} \text{ moly}^{-1}$
 134 (Müller & Stavrakou, 2004). For comparison, the amount of NO_x generated by the en-
 135 ergy deposited in a single impact with a large extraplanetary body can also be signif-
 136 icant, or overwhelming, with an estimated $1.25 \times 10^{10} \text{ mol}$ produced by the 1908 Tun-
 137 guska event (Curci et al., 2004) and $1.5 \times 10^{14} \text{ mol}$ by the Chicxulub impact 66 Ma (Parkos
 138 et al., 2015).

139 In this work, we present new experimental data simulating high-velocity impact
 140 shocks by laser-induced dielectric breakdown (LIDB) and probe the production of ni-
 141 trogen oxides. The measured production efficiency (or yield) of N_2O is applied to a pho-
 142 tochemical model of the Hadean atmosphere and the resultant steady-state abundance
 143 and greenhouse warming estimated.

144 2 Experimental yield of nitrogen oxides

145 2.1 Method

146 Terawatt-class laser-induced dielectric breakdown (TC-LIDB) of gas mixtures sim-
 147 ulating possible early-Earth atmospheric compositions was induced by the focused beam
 148 of the Prague Asterix Laser System (PALS) (Jungwirth et al., 2001) in a similar layout
 149 as used during previous studies performed in our laboratory, e.g., Civiš et al. (2004); Ferus
 150 et al. (2017); Ferus, Pietrucci, et al. (2019). The TW-class iodine photodissociation laser
 151 generates 350 ps pulses of 1315.2 nm near-infrared radiation and provides one pulse ev-
 152 ery 25 minutes. Each pulse can carry up to 1000 J of radiation energy. The laser beam
 153 was focused by a 15-cm-in-diameter CaF_2 plano-convex lens with a focal length of 25 cm
 154 through a 10 cm-diameter Pyrex window into a glass cell filled with the atmosphere ana-
 155 logue.

156 In multiphase experiments, the 800 cm^3 sample cell contains not only the gas mix-
 157 ture but also a liquid sample and/or catalytic solids representing planetary and mete-
 158 oritic materials. The height of the laser beam focus above this material is adjusted to
 159 avoid any direct interaction of the focused laser beam with solids and liquids (that is,
 160 the LIDB occurs in gas only) but to secure effective contact between the expanding LIDB
 161 plasma and condensed material.

162 During the experiments described here, a mixture of gases was typically subjected
 163 to between 11 and 25 pulses with 25 min pauses between subsequent pulses. The pulse
 164 energy was kept constant at 150 J, and the total accumulated energy varied between 1650
 165 to 3750 J. Each pulse interaction results in an expanding plasma mimicking the condi-
 166 tions surrounding a high-velocity extraterrestrial body as it enters the atmosphere, ex-
 167 plodes, or generates an impact plume. The analysis of atomic and molecular emission
 168 lines during our previous PALS TC-LIDB investigations revealed vibrational, rotational,
 169 and electronic excitation temperatures ranging from 4200 to 9300 K, depending on the
 170 sample composition and pressure and irradiation conditions (Babánková et al., 2006).
 171 In this study, the electron density has been estimated to reach 10^{17} cm^{-3} .

172 After each laser irradiation series, the gas-phase contents of the irradiation cell are
 173 transferred to a Bruker IFS 125HR high-resolution infrared Fourier-transform spectrom-
 174 eter for constituent analysis. The spectrometer was operated in the mid-infrared between
 175 600 and 4000 cm^{-1} using a KBr beamsplitter and HgCdTe liquid- N_2 -cooled detector. The

Table 1. Formation efficiencies and upper limits in laboratory LIDB experiments (molecules J^{-1}).

Sample composition ^a	NO	N ₂ O	NO ₂
N₂(80%), CO₂(20%)			
–	3.0×10^{16}	3.7×10^{16}	2.1×10^{15}
<i>v</i> (H ₂ O)	2.3×10^{16}	4.2×10^{14}	$< 3 \times 10^{14}$
<i>s</i> (anatase)	2.4×10^{16}	1.8×10^{16}	5.4×10^{14}
<i>v</i> (H ₂ O) <i>s</i> (clay)	1.8×10^{17}	4.2×10^{15}	8.8×10^{14}
<i>v</i> (HCl) <i>s</i> (clay)	8.6×10^{16}	2.0×10^{16}	5.8×10^{15}
<i>v</i> (HCl), <i>s</i> (anatase)	1.4×10^{16}	2.1×10^{16}	$< 3 \times 10^{15}$
<i>v</i> (H ₂ SO ₄), <i>s</i> (anatase)	8.8×10^{15}	3.6×10^{14}	$< 3 \times 10^{14}$
<i>v</i> (H ₂ SO ₄), <i>s</i> (anatase), <i>s</i> (clay)	5.0×10^{16}	$< 6 \times 10^{15}$	$< 6 \times 10^{15}$
<i>s</i> (anatase)	6.8×10^{16}	4.5×10^{15}	$< 6 \times 10^{14}$
<i>s</i> (anatase)	8.6×10^{16}	6.0×10^{15}	$< 2 \times 10^{15}$
CO(50%), NH₃(50%)			
–	2.3×10^{16}	2.8×10^{16}	$< 3 \times 10^{16}$
<i>v</i> (H ₂ O), <i>s</i> (clay)	2.6×10^{16}	1.9×10^{16}	$< 3 \times 10^{16}$
<i>v</i> (H ₂ O)	3.2×10^{16}	5.1×10^{16}	$< 2 \times 10^{15}$
<i>v</i> (H ₂ O), <i>s</i> (anatase)	1.2×10^{17}	1.2×10^{16}	$< 2 \times 10^{15}$
Mean yield	6×10^{16}	2×10^{16}	2×10^{15}

^aThe gas-phase composition is given in bold along with liquid / solution (*v*) and surface (*s*) samples present in the interaction chamber.

176 resulting spectra are averages of 200 measurements, apodised with a Blackman-Harris
177 function, and with a spectral resolution of 0.02 cm^{-1} . The concentrations of NO, NO₂
178 and N₂O were determined by comparison with calibration measurements over a wide range
179 of partial pressures using standard gases: nitrous oxide ($\geq 99.998\%$ purity, Sigma Aldrich),
180 nitric oxide (98.5%, Sigma Aldrich), nitrogen dioxide ($\geq 99.5\%$, Sigma Aldrich). A ver-
181 ification of this analysis was made by comparing the observed absorption band profiles
182 with simulations profiles computed from linelists taken from the HITRAN database (Gordon
183 et al., 2017). We analysed the NO fundamental band at 1875 cm^{-1} , NO₂ ν_3 band at 1618 cm^{-1} ,
184 and N₂O ν_3 band at 2224 cm^{-1} . The measured concentrations are converted into pro-
185 duction efficiencies, that is the amount of product formed per unit of input energy (molecules J^{-1}),
186 that can be used to scale our laser experiment to an impacted atmosphere.

187 The PALS laser deposits significantly greater energy than do tabletop LIDB facil-
188 ities, and generates a greater volume of hotter plasma, with measured electronic and vi-
189 brational temperatures $T_{\text{exc}} = 8000 - 10\,000 \text{ K}$ and $T_{\text{vib}} = 4200 - 6500 \text{ K}$. The chemi-
190 cally active plasma has a diameter of about 4 cm and the resulting fireball expands at
191 a velocity on the order of 300 km s^{-1} (Babánková et al., 2006; Ferus, Kubelík, et al., 2019).
192 The principal limitation of the PALS laser is its long 25 min duty cycle that precludes
193 the study of a wider range of sample compositions.

194

2.2 Results

195

196

197

198

199

200

201

202

203

204

205

206

207

208

The measured formation efficiencies for several models of the early Earth atmosphere are listed in Table 1 with NO and N₂O consistently detected and synthesised nitrogen oxide (NO₂) measured in several cases. All results are for 1 atm sample pressure with gas-phase composition corresponding to a redox-neutral atmosphere (N₂:CO₂ = 80:20) or reduced state (CO:NH₃ = 50:50). The elemental-nitrogen density is about three times greater in the former case, while the oxygen densities are similar. Additional experiments were conducted with each gas mixture including either liquid/solvent reservoirs (H₂O, HCl, H₂SO₄) or catalysing substrates (mineral anatase and montmorillonite clay). We have also reanalysed spectra taken from experimental campaigns conducted for various objectives (Civiš et al., 2004; Babánková et al., 2006; Civiš et al., 2008; Ferus et al., 2011; Ferus et al., 2014; Ferus et al., 2015; Civiš et al., 2016; Ferus et al., 2017; Ferus et al., 2017; Ferus, Pietrucci, et al., 2019). Regarding differences in yields of N₂O in particular mixtures with different gas phase and solid phase composition, we adopt for the model of planetary chemistry the mean production yield of each species.

209

210

211

212

213

214

215

The full range of measured NO production yields spans a factor of 20 with a mean of 6×10^{16} molec J⁻¹. The mean N₂O yield is 2×10^{16} molec J⁻¹ and varies by more than a factor of 100 between experiments, which reduces to a factor of 10 when neglecting two measurements with anomalously low N₂O yields below 10^{15} molec J⁻¹. A factor of 20 variation encompasses all measured NO₂ yields and upper limits, with a mean of 2×10^{15} molec J⁻¹. Only upper limits for NO₂ are available for the reducing-atmosphere CO:NH₃ experiments because of a strong overlap of NH₃ absorption with the NO₂ ν_3 band.

216

2.3 Discussion

217

218

219

220

221

A comparison of newly-measured yields with previous shock-chemistry experiments producing nitrogen oxides is given in Table 2 (see also the data reviewed in Lawrence et al. (1995) and Rahman and Cooray (2008)). Most existing data is collected in the interests of quantifying lightning-initiated nitrogen fixation in modern-Earth air, but some data exists for exotic gas mixtures and energy sources.

222

223

224

225

226

227

228

229

230

231

232

233

234

235

236

237

238

The NO yields in Table 2, or NO_x yields when NO is not discriminated from NO₂ but likely to be the dominant product, are generally consistent within a factor of ten and our measurement falls near the middle of their distribution. Significantly lower NO yields are measured when generated in a coronal discharge, which may be due to a higher degree of ionisation and lower temperature generated in these experiments relative to spark discharges and LIDB (Nna Mvondo et al., 2001). The measured 10^{16} to 5×10^{17} molec J⁻¹ NO yields are well-modelled by their thermochemical equilibrium abundance assuming a freeze-out temperature between 2000 to 5000 K in the rapidly cooling experimental plasmas and shocks (Chameides, 1979; Chameides & Walker, 1981; Mancinelli & McKay, 1988; Navarro-González et al., 2001). Their consistency persists over a large range of deposited energies (e.g., Table 1 of Cooray et al. (2009)); when generated by LIDB (e.g., Nna Mvondo et al. (2001); Navarro-González et al. (2001); Rahman and Cooray (2003)), pulsed lightning or coronal electric discharges (e.g., Levine et al. (1981); Stark et al. (1996); Nna Mvondo et al. (2001)), continuous plasma (Hill et al., 1988; Kim et al., 2010) or particle beams (Rahman et al., 2006). The NO yield is maximised for an approximately even N₂:CO₂ mixing ratio in the measurements of Nna Mvondo et al. (2001), which is also consistent with a low yield in the nitrogen-depleted Venus-analogue probed by Levine et al. (1982).

239

240

241

242

243

In experiments where the relative yield of NO and NO₂ is estimated, the production of the former is dominant. This is consistent with the 30:1 mean NO:NO₂ production ratio measured by us. In electric discharges, NO₂ may form after high-temperature shock conditions have dissipated from the NO primary-product (Chameides et al., 1977; Stark et al., 1996; Kim et al., 2010), and its abundance is enhanced by environmental

Table 2. Comparison of measured N_xO_y yields.

Simulated atmosphere	NO_x^a	Yield (molec. J^{-1})		N_2O	Reference
		NO	NO_2		
Experimental method: LIDB					
Early Earth ^b		6×10^{16}	2×10^{15}	2×10^{16}	This work ^c
Modern Earth		3×10^{14}			Navarro-González et al. (2001) ^d
Modern Earth		1.5×10^{17}			Navarro-González et al. (2001) ^e
Modern Earth	$(6.7 \pm 0.5) \times 10^{16}$	$(4.6 \pm 0.5) \times 10^{16}$			Rahman and Cooray (2003)
Early Mars ^f		4.1×10^{16}			Navarro-González et al. (2019)
Venus ^g		1.3×10^{16}			Nna Mvondo et al. (2001)
Experimental method: spark electric discharge					
Modern Earth	$(1.1 \pm 0.2) \times 10^{16}$				Cook et al. (2000)
Modern Earth		4.6×10^{17}			Wang et al. (1998)
Modern Earth	5×10^{15}				Stark et al. (1996)
Modern Earth	$1-2 \times 10^{16}$				Cooray and Rahman (2005) ^h
Modern Earth	$(6 \pm 1) \times 10^{16}$				Chameides et al. (1977)
Modern Earth	$(3.0 \pm 0.2) \times 10^{16}$	$(2.8 \pm 0.2) \times 10^{16}$			Rehbein and Cooray (2001)
Modern Earth				4×10^{12}	Levine et al. (1979)
Modern Earth		$(5 \pm 2) \times 10^{16}$			Levine et al. (1981)
Venus ⁱ		$(3.7 \pm 0.7) \times 10^{15}$			Levine et al. (1982)
Experimental method: coronal electric discharge					
Modern Earth	$3.6-5.7 \times 10^{14}$				Rehbein and Cooray (2001)
Early Earth ^j		1.3×10^{14}		1.2×10^{13}	Nna Mvondo et al. (2001)
Modern Earth		$(1.4 \pm 0.7) \times 10^{16}$		$(1.0 \pm 0.5) \times 10^{17}$	Hill et al. (1988) ^k
Experimental method: Sample flowed through a continuous microwave plasma					
Modern Earth		$0.5-0.8 \times 10^{16}$	$9-14 \times 10^{16}$		Kim et al. (2010)
Experimental method: Flowing sample subjected to α-particle irradiation					
Modern Earth		2×10^{17}			Rahman et al. (2006)

^a Odd-nitrogen species are not discriminated.^b $N_2 : CO_2 = 80 : 20$ or $CO : NH_3 = 50 : 50$ ^c The estimated uncertainty is a factor of 10.^d This is a partial yield measured in an expanding shock wave surrounding the laser-generated plasma.^e This is a partial yield measured in the core of laser-generated plasma.^f $CO_2 : N_2 : H_2 = 40 : 40 : 20$ ^g $N_2 : CO_2 = 20 : 80$ ^h In a positive-streamer discharge.ⁱ $N_2 : CO_2 = 4 : 96$ ^j Measured for a range of $N_2:CO_2$ mixing ratios, with the listed peak yields for a 1:1 mixture.^k Pulsed discharge in a flowing cell.

3 Nitrogen oxides in the Hadean atmosphere

3.1 Production rate

Laboratory measured and theoretically calculated N_xO_y chemical production efficiencies have been previously adapted to models of their impact production (e.g., Park (1978); Fegley et al. (1986); Prinn and Fegley (1987); Kasting (1990); Silber et al. (2018); Curci et al. (2004); Parkos et al. (2015); Navarro-González et al. (2019)). Theoretical and laboratory-informed computations of the primary NO yield aim to match the physical extremes and time scales occurring in the ablative or explosive shock wave generated by a descending impactor or its post-impact plume for a range of masses, compositions, velocities, and incidence angle. Photochemical and dynamical atmospheric models including surface deposition are needed to estimate the time-dependent abundance of NO_2 following an impact (e.g., Curci et al. (2004)), while the impact-formation of N_2O is not comprehensively studied.

Here, global impact-generated surface fluxes, Φ , of NO_2 , NO, and N_2O are computed directly from the mean yields, S , in Table 1 and assuming a steady impact-energy deposition rate, \dot{E}_T , and its efficient conversion into shock products. The surface flux of N_xO_y products is then

$$\Phi = \frac{S\dot{E}_T}{4\pi R^2} \quad (1)$$

where R is the Earth radius. We adopt properties of the late-heavy bombardment as summarised by Abramov et al. (2013). We assume impactors with a single velocity of 20 km s^{-1} deposit a total mass of $2 \times 10^{20} \text{ kg}$ over a period of 100 Myr. The average impact-energy deposition rate is then $1.3 \times 10^{13} \text{ J s}^{-1}$ and leads to NO, N_2O , and NO_2 surface fluxes of $\Phi = 1.5 \times 10^{11}$, 5×10^{10} , $5 \times 10^9 \text{ cm}^{-2} \text{ s}^{-1}$, respectively, under the assumption of complete conversion of impactor kinetic energy into an atmospheric shock. This latter assumption overestimates the calculated fluxes, with estimated conversion efficiencies (Chyba & Sagan, 1992) falling between 1 and 1/60, depending on the impactor mass and with the lowest efficiencies occurring for the largest impactors that also deliver most of the impactor energy.

The N_2O impact-generated surface flux is significantly larger than the $8.3 \times 10^3 \text{ cm}^{-2} \text{ s}^{-1}$ attributable to modern-day lightning (Schumann & Huntrieser, 2007). Chyba and Sagan (1992) estimate a $4.8 \times 10^{10} \text{ J s}^{-1}$ lightning and coronal-discharge energy dissipation rate at 4 Gya that corresponds to 300 times less N_2O produced than for the impact rate estimated here when assuming the same chemical formation efficiency.

3.2 Steady-state abundance

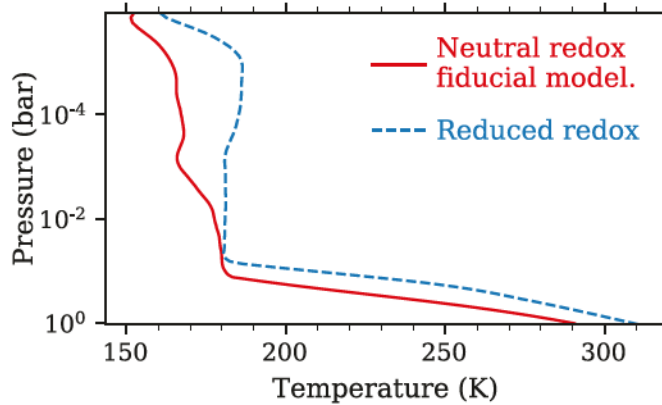
We estimate the lifetime of impact-generated nitrogen oxides in a model Hadean atmosphere with the ARGO one-dimensional Lagrangian photochemistry and diffusion program. This code and the accompanying STAND photochemical reaction network are designed for general planetary-atmosphere applications, have been described in detail elsewhere (Rimmer & Helling, 2016; Rimmer & Rugheimer, 2019), and previously applied to studies of lightning- and impact-induced chemistry of the early and modern Earth (Ardaseva et al., 2017; Ranjan et al., 2019; Rimmer et al., 2020). The ARGO model propagates a parcel of atmosphere from the surface to a maximum height and back again while time-integrating its photochemistry and partially mixing it with an initially-approximate ambient atmospheric composition at each vertical grid point traversed. The differential equation solved at each step is

$$\frac{dn_i}{dt} = P_i - L_i - \frac{\partial \Phi_i}{\partial x} \quad (2)$$

where n_i (cm^{-3}) is the height-dependent concentration of species i , P_i and L_i ($\text{cm}^{-3} \text{ s}^{-1}$) are its chemical production and loss rates, and Φ_i ($\text{cm}^{-2} \text{ s}^{-1}$) is the combined flux due

Table 3. Surface mixing ratio and modelled N₂O lifetimes.

Model	Surface mixing ratio						N ₂ O lifetime (y)
	N ₂	CO ₂	NH ₃	H ₂ O	H ₂	CO	
Neutral redox – fiducial model	0.8	0.2	0	0.01	10 ⁻³	10 ⁻⁵	2.2
Neutral redox – enhanced CO ₂	0.6	0.4	0	0.01	10 ⁻³	10 ⁻⁵	2.9
Neutral redox – reduced CO ₂	0.95	0.05	0	0.01	10 ⁻³	10 ⁻⁵	1.5
Reduced redox – NH ₃ /CO dominated	0	0	0.5	0.01	10 ⁻³	0.5	2.7

**Figure 2.** Temperature profile of the neutral redox and reduced atmosphere models.

309 to eddy and molecular diffusion. A height-independent eddy diffusion coefficient of
 310 $K = 10^5 \text{ cm}^2 \text{ s}^{-1}$ is adopted in all models presented here. By means of Eq. (2), diffu-
 311 sion is modelled in an efficient Lagrangian manner (Rimmer & Helling, 2016) and a steady
 312 state is reached between the propagated parcel and the atmospheric column after repeated
 313 traversals.

314 All models computed here have a 1 bar surface pressure and the major constituents
 315 of the fiducial case are N₂ and CO₂ in a 80:20 ratio. Fixed surface densities of the domi-
 316 nant species in this case, and for some comparative models, are listed in Table 3. The
 317 Hadean-eon solar photon flux at the top of the atmosphere is taken from the 3.8 Ga case
 318 computed by Claire et al. (2012) and as used by Rimmer et al. (2019). Fluxes longwards
 319 of 200 nm are reduced on average by 23% from the modern day, while shorter-wavelength
 320 radiation is progressively enhanced, reaching a factor of 5 by 100 nm. The pressure and
 321 temperature profiles are computed from a one-dimensional climate model as in Rimmer
 322 et al. (2019) and plotted in Fig. 2. The version of the STAND reaction network used here
 323 to compute kinetic and photolytic rates is described in Rimmer et al. (2021).

The computed densities of some species in the fiducial model are shown in Fig. 3
 neglecting the N_xO_y impact production. The N₂O density plotted in Fig. 3 is driven by
 its production from the reaction



324 NO in the impact-free model is, broadly speaking, the product of N₂O photodissocia-
 325 tion and is itself the precursor of NO₂, primarily through the reaction $\text{NO} + \text{HO}_2 \longrightarrow$
 326 $\text{NO}_2 + \text{OH}$.

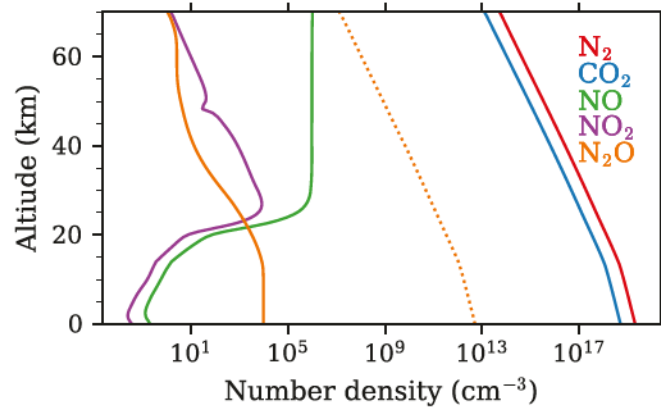


Figure 3. *Solid lines:* Densities computed by the fiducial atmospheric model with $\text{N}_2:\text{CO}_2=80:20$ and without impact formation. *Broken line:* An N_2O density of 200 ppb after consideration of its impact formation.

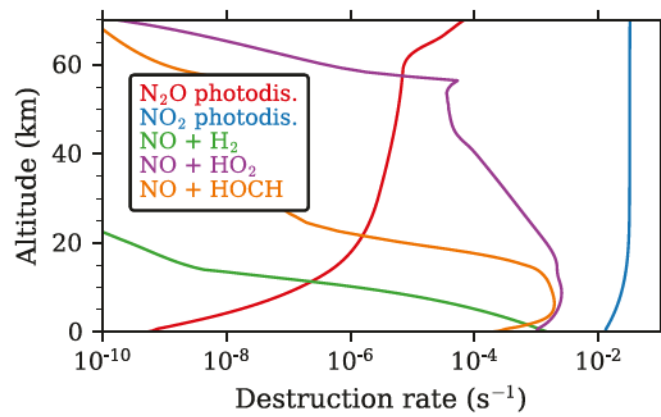


Figure 4. Dominant destruction mechanisms of NO , NO_2 , and N_2O in the neutral redox atmosphere.

If the photochemical destruction of continuously impact-generated N_xO_y species is irreversible, their steady-state column density sustained in the atmosphere is given by

$$N = \tau \times \Phi \quad (4)$$

where τ is a photochemical lifetime. The rates for the dominant processes destroying N_xO_y species computed with ARGO are plotted in Fig. 4, with N_2O being nominally more stable than NO or NO_2 . However, products of the leading NO and NO_2 destruction processes shown in Fig. 4 are, respectively, NO_2 and NO, forming a closed cycle that invalidates the use of Eq. (4). Instead, we assume that the rapid conversion of NO and NO_2 into HNO_2 and HNO_3 , followed by their dissolution and wet deposition is sufficient to eliminate these gases from the atmosphere such that no significant steady-state abundance is maintained, as is the case in the modern Earth atmosphere.

The photolysis of N_2O branches to produce both $N_2+O(^1S)$ and $N_2+O(^1D)$ but most metastable $O(^1D)$ is irreversibly collisionally de-excited before it can reform N_2O by Eq. (3), and we adopt Eq. (4) to estimate the equilibrium N_2O abundance. We make a simplifying assumption that the mixing ratio of impact-generated N_2O is independent of altitude. Then, the column-averaged N_2O destruction rate, J_{av} , computed from the photodissociation rate, $J(z)$, shown in Fig. 4 is

$$J_{av} = \frac{\int_0^{\text{top}} J(z)n(z) dz}{\int_0^{\text{top}} n(z) dz} \quad (5)$$

and corresponds to an average N_2O lifetime of 2.2 years in the fiducial model. This is significantly reduced from the 130 year lifetime of N_2O in the present-day atmosphere (Prather et al., 2012) which is greatly extended by ultraviolet shielding from O_2 and O_3 (Roberson et al., 2011). The equilibrium column density of impact-sourced N_2O according to Eq. (4) is then $4.0 \times 10^{19} \text{ cm}^{-2}$, corresponding to an average mixing ratio of 200 ppb. This is similar to the present-day mixing ratio of 300 ppb (Prather et al., 2012), despite the shortened lifetime, because of the sheer magnitude of the impact source term. The density of impact-generated N_2O thus computed is compared in Fig. 3 with its purely photochemical production.

A greater mixing ratio of N_2O could occur if its impact production predominantly occurs where it is effectively shielded from ultraviolet radiation, that is, below 20 km. In this case the $10^5 \text{ cm}^2 \text{ s}^{-1}$ eddy-diffusion coefficient adopted in our model implies a mixing timescale from the surface up to 20 km of about a year, such that the steady-state N_2O column density may increase by a factor of a few.

Further models with the CO_2 mixing ratio increased to 40% and decreased to 5% were used to compute further N_2O lifetimes, listed in Table 3. These lifetimes are affected by the presence of more or less ultraviolet shielding by CO_2 and vary within 40%. We also compute the N_2O destruction rate under the assumption of a reducing atmosphere with dominant components NH_3 and CO, as listed in Table 3, and find a 20% increased N_2O lifetime when assuming its mixing ratio to be height independent. This small change following a complete chemical substitution of the atmosphere arises from a balance between modelled N_2O photodissociation rates below 45 km and above, combined with its chemical destruction below 8 km by



as shown in Fig. 5. In the lower atmosphere, a multiple-orders-of-magnitude reduced photodissociation rate is the result of more effective shielding of N_2O photodissociation by NH_3 than by CO_2 in the primary model. At higher altitudes, the greater solar photolysis rate of NH_3 relative to CO_2 reduces its abundance dramatically and leaves N_2O unshielded. The location of N_2O impact production will then have a greater impact on its residence time in an NH_3 -rich atmosphere than for the $N_2 + CO_2$ case.

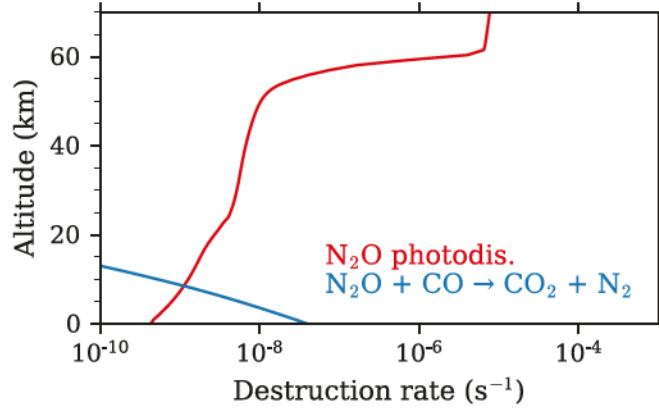


Figure 5. Dominant destruction mechanisms of N_2O in the reduced redox atmosphere.

355 Airapetian et al. (2016) compute the N_2O formation due to charged particles in-
 356 jected by flaring of the highly-active young Sun into an early-Earth atmosphere similar
 357 to the one modelled here (80% N_2 and 20% CO_2). They find the potential for an enhanced
 358 N_2O abundance well above our impact-estimate at altitudes above 30 km, but signifi-
 359 cant less below this and when integrated over the full atmospheric column.

360 3.3 N_2O greenhouse warming

361 Greenhouse warming in the modern atmosphere is sensitive to the N_2O abundance
 362 (Myhre et al., 2013) and Roberson et al. (2011) use a one-dimensional climate model to
 363 evaluate the warming potential of elevated levels of this molecule during the Protero-
 364 zoic, finding approximately 8 K climate warming following the addition of 30 ppm N_2O
 365 and 1 K of warming for 2 ppm. Byrne and Goldblatt (2014) computed radiative forcing
 366 for a range of greenhouse gases in an Archean atmosphere, and find good agreement with
 367 the climate model of Roberson et al. (2011) for an assumed climate sensitivity to N_2O
 368 consistent with the modern Earth. They also compute the reduction of N_2O radiative
 369 forcing due to its spectral overlap with CO_2 and CH_4 , finding approximately 33% reduc-
 370 tions for abundances of 10 000 and 100 ppm, respectively. The radiative forcing due to
 371 N_2O will be reduced further in our model Hadean atmosphere composed of 20% CO_2 ,
 372 but, in partial compensation, the N_2O lifetime is simultaneously increased from the ul-
 373 traviolet shielding of enhanced CO_2 and CH_4 .

374 A decrease of the 100 Myr duration of the LHB assumed in Sec. 3.1 will increase
 375 the production rate of N_2O and its warming potential. However, to achieve 1 K warm-
 376 ing, according to the Proterozoic climate model Roberson et al. (2011), an LHB span-
 377 ning only 10 Myr is needed, and would then have only a transient influence on the Hadean
 378 eon. Furthermore, an LHB extended in time is also possible, or a non-cataclysmic steadily-
 379 decreasing late accretion that deposits its energy (on average) more gradually. Our as-
 380 sumption in Sec. 3.1 of continuous energy deposition further overestimates the steady-
 381 state abundance N_2O , with most energy actually delivered episodically by large impacts
 382 (Abramov et al., 2013). A larger transient column density of N_2O than computed may
 383 then occur following a large impact, but its climatological influence would be likely over-
 384 shadowed by direct impact effects. In view of the above discussion it is clear that the
 385 excess of impact-generated N_2O computed here is insufficient to meaningfully warm the
 386 Hadean climate.

4 Conclusion

TC-LIDB chemistry initiated by a 150 J-per-pulse laser system is used as an analogue to the high-energy chemistry accompanying a meteor impact, and provides a better model of this process than small-scale LIDB experiments or high-temperature chemistry initiated by pulsed electric discharges. By post-analysing the products of shock chemistry we determine the final abundances of NO, N₂O, and NO₂ when probing two possible compositions of a Hadean-eon O₂-free atmosphere, 80% N₂ with 20% CO₂ and 50% CO with 50% NH₃. The NO and NO₂ yields in these anoxic mixtures are consistent with existing experimental data for the modern and early Earth. The measured N₂O yield falls between 4×10^{14} and 4×10^{16} molec J⁻¹ and is higher than implied by its non-detection in a tabletop LIDB experiment (Nna Mvondo et al., 2001), while previous electric-discharge yields are divergent (Levine et al., 1979; Hill et al., 1988).

We compute the steady-state abundance of N₂O in a photochemical model of an N₂ and CO₂ dominated Hadean atmosphere to be 200 ppb, when assuming an impact-generated N₂O flux consistent with a late-heavy bombardment of 100 Myr duration. The computed N₂O impact production rate far exceeds its generation by photochemical means or modern-day lightning production. The greenhouse warming attributable to the computed N₂O abundance is insufficient to raise the climatic temperature by a significant amount. Nonetheless, given the large N₂O yield found relative to other sources, the transient impact-generation of N₂O on the Hadean Earth or exoplanets undergoing heavy bombardment should be considered in comprehensive models of their chemistry and as a source of nitrogen fixation that may be significant for early-Earth and astrobiological prebiotic chemistry

Acknowledgments

This work is a part of a research series funded by grant no. 19-03314S of the Czech Science Foundation. The laboratory of high resolution spectroscopy acknowledges grant supporting equipment used in this study, ERDF/ESF “Centre of Advanced Applied Sciences” (No. CZ.02.1.01/0.0/0.0/16_019/0000778), and the Ministry of Education, Youth, and Sports of the Czech Republic (Project No. LM2018114). P. B. R. thanks the Simons Foundation for funding (SCOL awards 599634).

References

- Abramov, O., Kring, D. A., & Mojzsis, S. J. (2013). The impact environment of the Hadean Earth. *Geochem.*, *73*(3), 227 - 248. doi: 10.1016/j.chemer.2013.08.004
- Airapetian, V. S., Glocer, A., Gronoff, G., Hébrard, E., & Danchi, W. (2016, Jun). Prebiotic chemistry and atmospheric warming of early Earth by an active young Sun. *Nat. Geosci.*, *9*(6), 452-455. doi: 10.1038/ngeo2719
- Amend, J. P., & Shock, E. L. (2001, 04). Energetics of overall metabolic reactions of thermophilic and hyperthermophilic Archaea and Bacteria. *FEMS Microbiol. Rev.*, *25*(2), 175-243. Retrieved from <https://doi.org/10.1111/j.1574-6976.2001.tb00576.x> doi: 10.1111/j.1574-6976.2001.tb00576.x
- Ardaseva, A., Rimmer, P. B., Waldmann, I., Rocchetto, M., Yurchenko, S. N., Helling, C., & Tennyson, J. (2017, 05). Lightning chemistry on Earth-like exoplanets. *Monthly Notices of the Royal Astronomical Society*, *470*(1), 187-196. doi: 10.1093/mnras/stx1012
- Babánková, D., Civiš, S., Juha, L., Bittner, M., Cihelka, J., Pfeifer, M., ... Šedivcová, T. (2006, November). Optical and x-ray emission spectroscopy of high-power laser-induced dielectric breakdown in molecular gases and their mixtures. *J. Phys. Chem. A*, *110*(44), 12113-12120. doi: 10.1021/jp063689o
- Boehnke, P., & Harrison, T. M. (2016). Illusory late heavy bombardments. *Pro.*

- 436 *Natl. Acad. Sci.*, 113(39), 10802–10806. doi: 10.1073/pnas.1611535113
- 437 Bottke, W. F., & Norman, M. D. (2017). The late heavy bombardment. *Annu. Rev.*
438 *Earth Pl. Sc.*, 45(1), 619–647. doi: 10.1146/annurev-earth-063016-020131
- 439 Bottke, W. F., Vokrouhlický, D., Marchi, S., Swindle, T., Scott, E. R. D., Weirich,
440 J. R., & Levison, H. (2015). Dating the moon-forming impact event with aster-
441 oidal meteorites. *Science*, 348(6232), 321–323. doi: 10.1126/science.aaa0602
- 442 Buick, R. (2007). Did the Proterozoic ‘Canfield Ocean’ cause a laughing gas green-
443 house? *Geobiology*, 5(2), 97–100. doi: 10.1111/j.1472-4669.2007.00110.x
- 444 Byrne, B., & Goldblatt, C. (2014). Radiative forcings for 28 potential Archean
445 greenhouse gases. *Clim. Past*, 10(5), 1779–1801. doi: 10.5194/cp-10-1779-2014
- 446 Catling, D. C., & Zahnle, K. J. (2020). The archean atmosphere. *Sci. Adv.*, 6(9).
447 doi: 10.1126/sciadv.aax1420
- 448 Cavosie, A., Valley, J., Wilde, S., & E.I.M.F. (2005). Magmatic $\delta^{18}\text{O}$ in 4400–
449 3900 ma detrital zircons: A record of the alteration and recycling of crust
450 in the early archean. *Earth. Planet Sc. Lett.*, 235(3), 663 - 681. doi:
451 <https://doi.org/10.1016/j.epsl.2005.04.028>
- 452 Chameides, W. (1979). Effect of variable energy input on nitrogen-fixation in instan-
453 taneous linear discharges. *Nature*, 277(5692), 123–125. doi: 10.1038/277123a0
- 454 Chameides, W. L., Stedman, D. H., Dickerson, R. R., Rusch, D. W., & Cicerone,
455 R. J. (1977, 01). NO_x production in lightning. *J. Atmos. Sci.*, 34(1), 143–149.
456 doi: 10.1175/1520-0469(1977)034<0143:NPIL>2.0.CO;2
- 457 Chameides, W. L., & Walker, J. C. G. (1981, December). Rates of Fixation by
458 Lightning of Carbon and Nitrogen in Possible Primitive Atmospheres. *Origins*
459 *Life*, 11(4), 291–302. doi: 10.1007/BF00931483
- 460 Charnay, B., Wolf, E. T., Marty, B., & Forget, F. (2020, July). Is the faint young
461 sun problem for Earth solved? *Space Sci. Rev.*, 216(5), 90. doi: 10.1007/
462 s11214-020-00711-9
- 463 Chyba, C., & Sagan, C. (1992, January). Endogenous production, exogenous de-
464 livery and impact-shock synthesis of organic molecules: an inventory for the
465 origins of life. *Nature*, 355(6356), 125–132. doi: 10.1038/355125a0
- 466 Civiš, S., Ferus, M., Knížek, A., Kubelík, P., Kamas, M., Španěl, P., ... Civiš, S.
467 (2016). Spectroscopic investigations of high-energy-density plasma trans-
468 formations in a simulated early reducing atmosphere containing methane,
469 nitrogen and water. *Phys. Chem. Chem. Phys.*, 18, 27317–27325. doi:
470 10.1039/C6CP05025E
- 471 Civiš, S., Juha, L., Babánková, D., Cvačka, J., Frank, O., Jehlička, J., ... Ullschmied,
472 J. (2004). Amino acid formation induced by high-power laser in $\text{CO}_2/\text{CO}-$
473 $\text{N}_2-\text{H}_2\text{O}$ gas mixtures. *Chem. Phys. Lett.*, 386(1), 169. doi: [https://doi.org/](https://doi.org/10.1016/j.cplett.2004.01.034)
474 [10.1016/j.cplett.2004.01.034](https://doi.org/10.1016/j.cplett.2004.01.034)
- 475 Civiš, S., Babánková, D., Cihelka, J., Sazama, P., & Juha, L. (2008, August). Spec-
476 troscopic investigations of high-power laser-induced dielectric breakdown in gas
477 mixtures containing carbon monoxide. *J. Phys. Chem. A*, 112(31), 7162–7169.
478 doi: 10.1021/jp712011t
- 479 Claire, M. W., Sheets, J., Cohen, M., Ribas, I., Meadows, V. S., & Catling, D. C.
480 (2012, sep). The evolution of solar flux from 0.1 nm to 160 μm : Quan-
481 titative estimates for planetary studies. *Astrophys. J.*, 757(1), 95. doi:
482 10.1088/0004-637x/757/1/95
- 483 Cook, D. R., Liaw, Y. P., Sisterson, D. L., & Miller, N. L. (2000, March). Produc-
484 tion of nitrogen oxides by a large spark generator. *J. Geophys. Res.*, 105(D6),
485 7103–7110. doi: 10.1029/1999JD901138
- 486 Cooray, V., & Rahman, M. (2005). Efficiencies for production of NO_x and O_3 by
487 streamer discharges in air at atmospheric pressure. *J. Electrostat.*, 63(6), 977 -
488 983. (10th International Conference on Electrostatics) doi: [https://doi.org/10](https://doi.org/10.1016/j.elstat.2005.03.071)
489 [.1016/j.elstat.2005.03.071](https://doi.org/10.1016/j.elstat.2005.03.071)
- 490 Cooray, V., Rahman, M., & Rakov, V. (2009). On the NO_x production by labora-

- 491 tory electrical discharges and lightning. *J. Atmos. Sol.-Terr. Phys.*, 71(17), 1877
 492 - 1889. doi: 10.1016/j.jastp.2009.07.009
- 493 Curci, G., Visconti, G., Jacob, D. J., & Evans, M. J. (2004, March). Tropospheric
 494 fate of Tunguska generated nitrogen oxides. *Geophys. Res. Lett.*, 31(6),
 495 L06123. doi: 10.1029/2003GL019184
- 496 Donohoe, K., Shair, F., & Wulf, O. (1977). Production of O₃, NO, and N₂O in a
 497 pulsed discharge at 1 atm. *Ind. Eng. Chem. Fundamen.*, 16(2), 208-215. doi:
 498 10.1021/i160062a006
- 499 Ducluzeau, A.-L., van Lis, R., Duval, S., Schoepp-Cothenet, B., Russell, M. J., &
 500 Nitschke, W. (2009). Was nitric oxide the first deep electron sink? *Trends*
 501 *Biochem. Sci.*, 34(1), 9 - 15. doi: 10.1016/j.tibs.2008.10.005
- 502 Fegley, J., B., Prinn, R. G., Hartman, H., & Watkins, G. H. (1986, January). Chem-
 503 ical effects of large impacts on the Earth's primitive atmosphere. *Nature*,
 504 319(6051), 305-308. doi: 10.1038/319305a0
- 505 Ferus, M., Kubelík, P., Knížek, A., Pastorek, A., Sutherland, J., & Civiš, S. (2017,
 506 Jul). High energy radical chemistry formation of HCN-rich atmospheres on
 507 early Earth. *Sci. Rep.-UK*, 7, 6275. doi: 10.1038/s41598-017-06489-1
- 508 Ferus, M., Kubelík, P., Petera, L., Lenza, L., Koukal, J., Krivková, A., ... Krus,
 509 M. (2019). Main spectral features of meteors studied using a terawatt-class
 510 high-power laser. *Astron. Astrophys.*, 630, A127. doi: 10.1051/0004-6361/
 511 201935816
- 512 Ferus, M., Kubelík, P., & Civiš, S. (2011). Laser spark formamide decomposition
 513 studied by FT-IR spectroscopy. *J. Phys. Chem. A*, 115(44), 12132-12141. doi:
 514 10.1021/jp205413d
- 515 Ferus, M., Michalčíková, R., Shestivská, V., Šponer, J., Šponer, J. E., & Civiš,
 516 S. (2014, January). High-energy chemistry of formamide: A simpler
 517 way for nucleobase formation. *J. Phys. Chem. A*, 118(4), 719-736. doi:
 518 10.1021/jp411415p
- 519 Ferus, M., Nesvorný, D., Šponer, J., Kubelík, P., Michalčíková, R., Shestivská, V.,
 520 ... Civiš, S. (2015). High-energy chemistry of formamide: A unified mecha-
 521 nism of nucleobase formation. *Pro. Natl. Acad. Sci.*, 112(3), 657-662. doi:
 522 10.1073/pnas.1412072111
- 523 Ferus, M., Pietrucci, F., Saitta, A. M., Ivanek, O., Knizek, A., Kubelí, ... Cas-
 524 sone, G. (2019). Prebiotic synthesis initiated in formaldehyde by laser
 525 plasma simulating high-velocity impacts. *Astron. Astrophys.*, 626, A52.
 526 Retrieved from <https://doi.org/10.1051/0004-6361/201935435> doi:
 527 10.1051/0004-6361/201935435
- 528 Ferus, M., Pietrucci, F., Saitta, A. M., Knížek, A., Kubelík, P., Ivanek, O., ... Civiš,
 529 S. (2017). Formation of nucleobases in a Miller-Urey reducing atmosphere.
 530 *Pro. Natl. Acad. Sci.*, 114(17), 4306-4311. doi: 10.1073/pnas.1700010114
- 531 Feulner, G. (2012). The faint young Sun problem. *Rev. Geophys.*, 50(2). doi: 10
 532 .1029/2011RG000375
- 533 Genda, H., Brasser, R., & Mojzsis, S. (2017). The terrestrial late veneer from core
 534 disruption of a lunar-sized impactor. *Earth. Planet Sc. Lett.*, 480, 25 - 32. doi:
 535 <https://doi.org/10.1016/j.epsl.2017.09.041>
- 536 Glarborg, P., Miller, J. A., Ruscic, B., & Klippenstein, S. J. (2018). Modeling nitro-
 537 gen chemistry in combustion. *Prog. Energy. Combust. Sci.*, 67, 31 - 68. doi:
 538 <https://doi.org/10.1016/j.pecs.2018.01.002>
- 539 Gordon, I., Rothman, L., Hill, C., Kochanov, R., Tan, Y., Bernath, P., ... Zak, E.
 540 (2017). The HITRAN2016 molecular spectroscopic database. *J. Quant.*
 541 *Spectrosc. Radiat. Transfer*, 203, 3 - 69. (HITRAN2016 Special Issue) doi:
 542 <https://doi.org/10.1016/j.jqsrt.2017.06.038>
- 543 Gribaldo, S., Talla, E., & Brochier-Armanet, C. (2009). Evolution of the haem
 544 copper oxidases superfamily: a rooting tale. *Trends Biochem. Sci.*, 34(8), 375 -
 545 381. doi: 10.1016/j.tibs.2009.04.002

- 546 Haqq-Misra, J. D., Domagal-Goldman, S. D., Kasting, P. J., & Kasting, J. F.
 547 (2008). A revised, hazy methane greenhouse for the Archean Earth. *Astro-*
 548 *biology*, 8(6), 1127-1137. doi: 10.1089/ast.2007.0197
- 549 Hill, R., Rahmin, I., & Rinker, R. (1988, JUL). Experimental-study of the pro-
 550 duction of NO, N₂O, and O₃ in a simulated atmospheric corona [Article]. *Ind.*
 551 *Eng. Chem. Res.*, 27(7), 1264. doi: 10.1021/ie00079a029
- 552 Hill, R., Rinker, R., & Coucouvinos, A. (1984). Nitrous-oxide production
 553 by lightning. *J. Geophys. Res. – Atmos.*, 89(ND1), 1411-1421. doi:
 554 10.1029/JD089iD01p01411
- 555 Jungwirth, K., Cejnarova, A., Juha, L., Kralikova, B., Krasa, J., Krousky, E., ...
 556 Ullschmied, J. (2001). The Prague Asterix Laser System. *Physics of Plasmas*,
 557 8(5), 2495-2501. doi: 10.1063/1.1350569
- 558 Kasting, J. F. (1990). Bolide impacts and the oxidation-state of carbon in the
 559 Earths early atmosphere. *Origins. Life. Evol. B.*, 20(3-4), 199. (1989 meeting
 560 of the international soc for the study of the origin of life, Prague, czechoslo-
 561 vakkia, 1989) doi: 10.1007/BF01808105
- 562 Kasting, J. F. (2014, 05). Atmospheric composition of Hadean-early Archean Earth:
 563 The importance of CO. In *Earth's Early Atmosphere and Surface Environment*
 564 (p. 19-28). Geological Society of America. doi: 10.1130/2014.2504(04)
- 565 Kasting, J. F., & Catling, D. (2003). Evolution of a habitable planet. *Annu.*
 566 *Rev. Astron. Astrophys.*, 41(1), 429-463. doi: 10.1146/annurev.astro.41.071601
 567 .170049
- 568 Kiehl, J. T., & Dickinson, R. E. (1987). A study of the radiative effects of enhanced
 569 atmospheric CO₂ and CH₄ on early Earth surface temperatures. *J. Geophys.*
 570 *Res. – Atmos.*, 92(D3), 2991-2998. doi: 10.1029/JD092iD03p02991
- 571 Kim, T., Song, S., Kim, J., & Iwasaki, R. (2010, dec). Formation of NO_x from
 572 air and N₂/O₂ mixtures using a nonthermal microwave plasma system. *Jpn. J.*
 573 *Appl. Phys.*, 49(12), 126201. doi: 10.1143/jjap.49.126201
- 574 Koeberl, C. (2006, 08). Impact processes on the early Earth. *Elements*, 2(4), 211-
 575 216. doi: 10.2113/gselements.2.4.211
- 576 Koeberl, C., Reimold, W., McDonald, I., & Rosing, M. (2000). Impacts and the
 577 Early Earth. Lecture Notes in Earth Sciences. In (p. 73-97). Springer, Berlin,
 578 Heidelberg. doi: 10.1007/BFb0027757
- 579 Kuhn, W. R., & Kasting, J. F. (1983, Jan). Effects of increased CO₂ concentrations
 580 on surface temperature of the early Earth. *Icarus*, 301, 53-55. doi: 10.1038/
 581 301053a0
- 582 Kuwahara, H., & Sugita, S. (2015). The molecular composition of impact-generated
 583 atmospheres on terrestrial planets during the post-accretion stage. *Icarus*, 257,
 584 290 - 301. doi: <https://doi.org/10.1016/j.icarus.2015.05.007>
- 585 Lammer, H., Zerkle, A. L., Gebauer, S., Tosi, N., Noack, L., Scherf, M., ... Nikolaou,
 586 A. (2018, MAY 10). Origin and evolution of the atmospheres of early Venus,
 587 Earth and Mars. *Astron. Astrophys. Rev.*, 26. doi: 10.1007/s00159-018-0108-y
- 588 Lawrence, M. G., Chameides, W. L., Kasibhatla, P. S., Levy, H., & Moxim, W.
 589 (1995). Handbook of atmospheric electrodynamics. In (p. 189-202). University
 590 of Bon. doi: 10.1007/978-1-4419-1684-6_2
- 591 Levine, J. S., Gregory, G. L., Harvey, G. A., Howell, W. E., Borucki, W. J., &
 592 Orville, R. E. (1982, August). Production of nitric oxide by lightning on
 593 Venus. *Geophys. Res. Lett.*, 9(8), 893-896. doi: 10.1029/GL009i008p00893
- 594 Levine, J. S., Hughes, R. E., Chameides, W. L., & Howell, W. E. (1979). N₂O and
 595 CO production by electric-discharge: Atmospheric implications. *Geophys. Res.*
 596 *Lett.*, 6(7), 557. doi: 10.1029/GL006i007p00557
- 597 Levine, J. S., Rogowski, R. S., Gregory, G. L., Howell, W. E., & Fishman, J. (1981).
 598 Simultaneous measurements of NO_x, NO, and O₃ production in a laboratory
 599 discharge: Atmospheric implications. *Geophys. Res. Lett.*, 8(4), 357-360. doi:
 600 10.1029/GL008i004p00357

- 601 Lock, S. J., Bermingham, K. R., Parai, R., & Boyet, M. (2020, September).
 602 Geochemical constraints on the origin of the Moon and preservation of
 603 ancient terrestrial heterogeneities. *Space Sci. Rev.*, 216(6), 109. doi:
 604 10.1007/s11214-020-00729-z
- 605 Mancinelli, R. L., & McKay, C. P. (1988, Dec 01). The evolution of nitrogen cycling.
 606 *Origins Life Evol. Biosphere*, 18(4), 311–325. doi: 10.1007/BF01808213
- 607 Marchi, S., Bottke, W. F., Elkins-Tanton, L. T., Bierhaus, M., Wuenemann, K.,
 608 Morbidelli, A., & Kring, D. A. (2014, July). Widespread mixing and burial of
 609 Earth’s Hadean crust by asteroid impacts. *Nature*, 511(7511), 578–582. doi:
 610 10.1038/nature13539
- 611 Mojzsis, S. J., Brasser, R., Kelly, N. M., Abramov, O., & Werner, S. C. (2019, aug).
 612 Onset of giant planet migration before 4480 million years ago. *Astrophys. J.*,
 613 881(1), 44. doi: 10.3847/1538-4357/ab2c03
- 614 Morbidelli, A., Nesvorný, D., Laurenz, V., Marchi, S., Rubie, D., Elkins-Tanton, L.,
 615 ... Jacobson, S. (2018). The timeline of the lunar bombardment: Revisited.
 616 *Icarus*, 305, 262 - 276. doi: <https://doi.org/10.1016/j.icarus.2017.12.046>
- 617 Müller, J. F., & Stavrakou, T. (2004, December). Inversion of CO and NO_x emis-
 618 sions using the adjoint of the IMAGES model. *Atmos. Chem. Phys.*, 4(6),
 619 7985–8068. doi: 10.5194/acpd-4-7985-2004
- 620 Myhre, G., Shindell, D., Bréon, F.-M., Collins, W., Fuglestedt, J., Huang, J., ...
 621 Zhang, H. (2013). Climate change 2013: The physical science basis. contribu-
 622 tion of working group I to the fifth assessment report of the intergovernmental
 623 panel on climate change. In (p. 659-740). Cambridge University Press.
- 624 Navarro-González, R., Villagrán-Muniz, M., Sobral, H., Molina, L. T., & Molina,
 625 M. J. (2001). The physical mechanism of nitric oxide formation in sim-
 626 ulated lightning. *Geophys. Res. Lett.*, 28(20), 3867–3870. doi: 10.1029/
 627 2001GL013170
- 628 Navarro-González, R., Navarro, K. F., Coll, P., McKay, C. P., Stern, J. C., Sut-
 629 ter, B., ... Vasavada, A. R. (2019). Abiotic input of fixed nitrogen by
 630 bolide impacts to Gale Crater during the Hesperian: Insights from the
 631 Mars science laboratory. *J. Geophys. Res. – Planet.*, 124(1), 94–113. doi:
 632 10.1029/2018JE005852
- 633 Nna Mvondo, D., Navarro-Gonzalez, R., McKay, C., Coll, P., & Raulin, F. (2001).
 634 Production of nitrogen oxides by lightning and coronae discharges in simulated
 635 early Earth, Venus and Mars environments. In Raulin, F and Kobayashi, K
 636 and Brack, A and Greensberg, JM and Hei, TK (Ed.), *Space life sciences: Life
 637 in the Solar system: Prebiotic chemistry, chirality and space biology* (Vol. 27,
 638 p. 217–223).
- 639 Park, C. (1978). Nitric oxide production by Tunguska meteor. *Acta Astronaut.*, 5(7),
 640 523 - 542. doi: [https://doi.org/10.1016/0094-5765\(78\)90082-6](https://doi.org/10.1016/0094-5765(78)90082-6)
- 641 Parkos, D., Alexeenko, A., Kulakhmetov, M., Johnson, B. C., & Melosh, H. J.
 642 (2015). NO_x production and rainout from Chicxulub impact ejecta reentry. *J.
 643 Geophys. Res. – Planet.*, 120(12), 2152–2168. doi: 10.1002/2015JE004857
- 644 Prather, M. J., Holmes, C. D., & Hsu, J. (2012). Reactive greenhouse gas scenarios:
 645 Systematic exploration of uncertainties and the role of atmospheric chemistry.
 646 *Geophys. Res. Lett.*, 39(9). doi: 10.1029/2012GL051440
- 647 Prinn, R. G., & Fegley, B. (1987). Bolide impacts, acid rain, and biospheric trau-
 648 mas at the Cretaceous-Tertiary boundary. *Earth. Planet Sc. Lett.*, 83(1), 1 -
 649 15. doi: [https://doi.org/10.1016/0012-821X\(87\)90046-X](https://doi.org/10.1016/0012-821X(87)90046-X)
- 650 Rahman, M., & Cooray, V. (2003). NO_x generation in laser-produced plasma in air
 651 as a function of dissipated energy. *Opt. Laser Technol.*, 35(7), 543 - 546. doi:
 652 [https://doi.org/10.1016/S0030-3992\(03\)00077-X](https://doi.org/10.1016/S0030-3992(03)00077-X)
- 653 Rahman, M., & Cooray, V. (2008). A study of NO_x production in air heated by
 654 laser discharges: Effect of energy, wavelength, multiple discharges and pres-
 655 sure. *Opt. Laser Technol.*, 40(1), 208 - 214. doi: 10.1016/j.optlastec.2007.01

- 556 .007
- 557 Rahman, M., Cooray, V., Possnert, G., & Nyberg, J. (2006). An experi-
 558 mental quantification of the NO_x production efficiency of energetic al-
 559 pha particles in air. *J. Atmos. Sol.-Terr. Phys.*, 68(11), 1215 - 1218. doi:
 560 <https://doi.org/10.1016/j.jastp.2006.03.003>
- 561 Ranjan, S., Todd, Z. R., Rimmer, P. B., Sasselov, D. D., & Babbin, A. R. (2019).
 562 Nitrogen oxide concentrations in natural waters on early Earth. *Geochem.*
 563 *Geophys. Geosy.*, 20(4), 2021-2039. doi: 10.1029/2018GC008082
- 564 Rehbein, N., & Cooray, V. (2001). NO_x production in spark and corona discharges.
 565 *J. Electrostat.*, 51-52, 333 - 339. (Electrostatics 2001: 9th International Confer-
 566 ence on Electrostatics) doi: [https://doi.org/10.1016/S0304-3886\(01\)00115-2](https://doi.org/10.1016/S0304-3886(01)00115-2)
- 567 Rimmer, P. B., Ferus, M., Waldmann, I. P., Knizek, A., Kalvaitis, D., Ivanek, O., ...
 568 Granville-Willett, A. (2020, JAN 1). Identifiable acetylene features predicted
 569 for young Earth-like exoplanets with reducing atmospheres undergoing heavy
 570 bombardment [Article]. *Astrophys. J.*, 888(1). doi: 10.3847/1538-4357/ab55e8
- 571 Rimmer, P. B., & Helling, C. (2016, may). A chemical kinetics network for lightning
 572 and life in planetary atmospheres. *Astrophys. J. Suppl. Ser.*, 224(1), 9. doi: 10
 573 .3847/0067-0049/224/1/9
- 574 Rimmer, P. B., Jordan, S., Constantinou, T., Woitke, P., Shorttle, O., Hobbs, R., &
 575 Paschodimas, A. (2021). three different ways to explain the sulfur depletion in
 576 the clouds of Venus. *In preparation*.
- 577 Rimmer, P. B., & Rugheimer, S. (2019). Hydrogen cyanide in nitrogen-rich atmo-
 578 spheres of rocky exoplanets. *Icarus*, 329, 124 - 131. doi: [https://doi.org/10](https://doi.org/10.1016/j.icarus.2019.02.020)
 579 .1016/j.icarus.2019.02.020
- 580 Rimmer, P. B., Shorttle, O., & Rugheimer, S. (2019). Oxidised micrometeorites as
 581 evidence for low atmospheric pressure on the early Earth. *Geochem. Perspect.*
 582 *Lett.*, 9, 38-42. doi: 10.7185/geochemlet.1903
- 583 Roberson, A. L., Roadt, J., Halevy, I., & Kasting, J. F. (2011). Greenhouse warming
 584 by nitrous oxide and methane in the Proterozoic Eon. *Geobiology*, 9(4), 313-
 585 320. doi: 10.1111/j.1472-4669.2011.00286.x
- 586 Ryder, G. (2002, April). Mass flux in the ancient Earth-Moon system and be-
 587 nign implications for the origin of life on Earth. *J. Geophys. Res. - Planet.*,
 588 107(E4), 5022. doi: 10.1029/2001JE001583
- 589 Sagan, C., & Mullen, G. (1972). Earth and mars: Evolution of atmospheres and sur-
 590 face temperatures. *Science*, 177(4043), 52-56.
- 591 Schumann, U., & Huntrieser, H. (2007, July). The global lightning-induced nitrogen
 592 oxides source. *Atmos. Chem. Phys.*, 7(14), 3823-3907.
- 593 Shaw, G. H. (2008). Earth's atmosphere - Hadean to early Proterozoic. *Geochem.*,
 594 68(3), 235 - 264. doi: <https://doi.org/10.1016/j.chemer.2008.05.001>
- 595 Silber, E. A., Niculescu, M. L., Butka, P., & Silber, R. E. (2018, MAY). Nitric
 596 oxide production by centimeter-sized meteoroids and the role of linear and
 597 nonlinear processes in the shock bound flow fields. *Atmosphere*, 9(5). doi:
 598 10.3390/atmos9050202
- 599 Stanton, C. L., Reinhard, C. T., Kasting, J. F., Ostrom, N. E., Haslun, J. A., Lyons,
 700 T. W., & Glass, J. B. (2018). Nitrous oxide from chemodenitrification: A pos-
 701 sible missing link in the Proterozoic greenhouse and the evolution of aerobic
 702 respiration. *Geobiology*, 16(6), 597-609. doi: 10.1111/gbi.12311
- 703 Stark, M. S., Harrison, J. T. H., & Anastasi, C. (1996). Formation of nitrogen oxides
 704 by electrical discharges and implications for atmospheric lightning. *J. Geophys.*
 705 *Res. - Atmos.*, 101(D3), 6963-6969. doi: 10.1029/95JD03008
- 706 Taillades, J., Collet, H., Garrel, L., Beuzelin, I., Boiteau, L., Choukroun, H., &
 707 Commeyras, A. (1999, JUN). N-carbamoyl amino acid solid-gas nitro-
 708 sation by NO/NO_x: A new route to oligopeptides via alpha-amino acid N-
 709 carboxyanhydride. Prebiotic implications. *J. Mol. Evol.*, 48(6), 638-645. doi:
 710 10.1007/PL00006507

- 711 Wang, Y., DeSilva, A. W., Goldenbaum, G. C., & Dickerson, R. R. (1998). Ni-
712 tric oxide production by simulated lightning: Dependence on current, en-
713 ergy, and pressure. *J. Geophys. Res. – Atmos.*, *103*(D15), 19149-19159. doi:
714 10.1029/98JD01356
- 715 Wetherill, G. W. (1975, January). Late heavy bombardment of the moon and terres-
716 trial planets. *Proc. Lunar. Planet. Sci.*, *2*, 1539-1561.
- 717 Wilde, S., Valley, J., Peck, W., & Graham, C. (2001, JAN 11). Evidence from de-
718 trital zircons for the existence of continental crust and oceans on the Earth 4.4
719 Gyr ago. *Nature*, *409*(6817), 175-178. doi: 10.1038/35051550
- 720 Wong, M. L., Charnay, B. D., Gao, P., Yung, Y. L., & Russell, M. J. (2017). Ni-
721 trogen oxides in early Earth’s atmosphere as electron acceptors for life’s emer-
722 gence. *Astrobiology*, *17*(10), 975-983. doi: 10.1089/ast.2016.1473
- 723 Yang, X., Gaillard, F., & Scaillet, B. (2014). A relatively reduced Hadean con-
724 tinental crust and implications for the early atmosphere and crustal rheol-
725 ogy. *Earth. Planet Sc. Lett.*, *393*, 210 - 219. doi: [https://doi.org/10.1016/](https://doi.org/10.1016/j.epsl.2014.02.056)
726 [j.epsl.2014.02.056](https://doi.org/10.1016/j.epsl.2014.02.056)
- 727 Zahnle, K. J., Lupu, R., Catling, D. C., & Wogan, N. (2020, may). Creation and
728 evolution of impact-generated reduced atmospheres of early Earth. *Planet. Sci.*
729 *J.*, *1*(1), 11. doi: 10.3847/psj/ab7e2c